

# Physics Informed Neural Network using Finite Difference Method

Kart Leong Lim, Rahul Dutta, Mihai Rotaru

**Abstract**—In recent engineering applications using deep learning, physics-informed neural network (PINN) is a new development as it can exploit the underlying physics of engineering systems. The novelty of PINN lies in the use of partial differential equations (PDE) for the loss function. Most PINNs are implemented using automatic differentiation (AD) for training the PDE loss functions. A lesser well-known study is the use of finite difference method (FDM) as an alternative. Unlike an AD based PINN, an immediate benefit of using a FDM based PINN is low implementation cost. In this paper, we propose the use of finite difference method for estimating the PDE loss functions in PINN. Our work is inspired by computational analysis in electromagnetic systems that traditionally solve Laplace’s equation using successive over-relaxation. In the case of Laplace’s equation, our PINN approach can be seen as taking the Laplacian filter response of the neural network output as the loss function. Thus, the implementation of PINN can be very simple. In our experiments, we tested PINN on Laplace’s equation and Burger’s equation. We showed that using FDM, PINN consistently outperforms non-PINN based deep learning. When comparing to AD based PINNs, we showed that our method is faster to compute as well as on par in terms of error reduction.

## I. INTRODUCTION

Recent advancement in multiphysics modeling combines deep learning with partial differential equations (PDEs), through the use of modern deep learning tools. The physics-informed neural network (PINN) [1] play such a role by constraining the data-driven neural network with physics laws. A key aspect of PINN is the use of automatic differentiation (AD) which compute partial derivatives of the neural network, allowing PDEs to seamlessly backpropagate through neural network [1], [2], [3], [4], [5], [6]. This physics-awareness [7] which transits from physics law to weight update allows neural network to better generalize real-world problem. An awareness that is unlikely to be picked up by past data-centric deep learning approaches such as ResNet [8]. Till date, PINNs are seen in fluid mechanics [1], heat transfer [9], contaminant transport [10], shock hydrodynamics and electromagnetic field [11].

Despite the success of using AD in PINN, some researchers [12], [13] have contemplated AD as a black-box solver and brought up several concerns. Problems arising from AD based PINN includes:

- i) Having lower accuracies when smaller collocation points are used [13] and longer computational time.
- ii) Seldom shown theoretically to converge [12].

To the best of our knowledge, only a handful of numerical differentiation (ND) themed PINN exists. They include: a)

PINN using finite volume method [12], b) PINN which combines automatic difference with finite difference [13], c) control volume PINN [7] and the finite volume PINN [10]. To distinguish between these PINNs, we group the former [13], [12] as PINNs which discard automatic differentiation from the training of PINN entirely while the latter [10], [7] are PINNs that incorporate NDs into the loss functions but will require automatic differentiation to work.

Our task is mainly targeted at exploring numerical differentiation as an alternative to automatic differentiation for the PINN loss function (i.e. following the works of [13], [12]). We quantify this task assessment by measuring the efficiency of PINNs under fewer collocation points and comparing the computational cost. Our approach is inspired by electromagnetic analysis that uses finite difference method (FDM) to approximate PDEs. We first disjoint the PDE solver from the loss function of PINN, simplifying our task. The PDE solver can be as simple as averaging the neighborhood of a node. In the case of Laplace’s equation, our PDE solver using FDM mimics the residual node response of electromagnetic system and resembles the Laplacian filter in image processing. Using chain rule, the PINN loss function can be re-assembled back and can be trained completely without requiring AD. We called our method as the FDM based PINN (FDM-PINN).

In our experiment, we applied FDM-PINN to the rectangular conducting trough problem which uses Laplace’s equation and the classical case of PINN using Burger’s equation. We compared our approach to both the AD based PINN and a regular neural network or NN. Our results showed that FDM-PINN outperforms NN in terms of lower error. Also, FDM-PINN does not require a GPU to compute, yet is on par or outperforms the AD based PINN at low collocation points conditions and is computational faster.

To our best knowledge, the only relevant work to FDM-PINN is can-PINN [13]. The main difference being can-PINN is a hybrid solution that first requires automatic differentiation to compute the PDE loss i.e.  $\delta u/\delta x$  (where  $u$  is the neural network output) before applying numerical differentiation on  $\delta u/\delta x$  to augment PINN. Furthermore, can-PINN is only tested on first-order PDE problems. In our case, we are completely automatic differentiation free when training the PDE loss of PINN. This is possible by introducing a PDE solver [14] to the PDE loss of PINN as discussed in Section III.C.

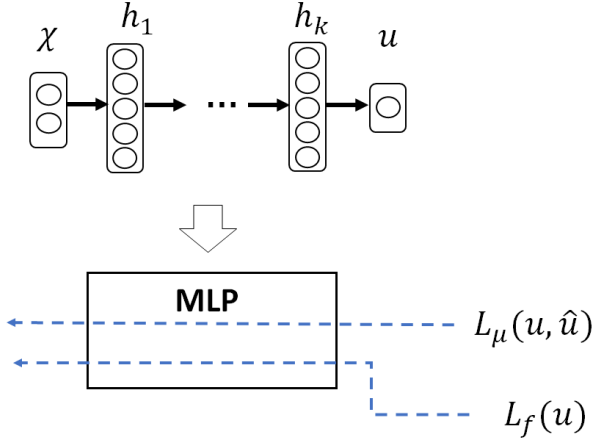


Figure 1. PINN is trained using mean square error loss  $L_\mu$  (data-driven) and physics-informed loss  $L_f$  (data-free). The architecture of PINN uses a MLP.

## II. BACKGROUND ON PINN

In recent engineering applications using deep learning, physics-informed neural network (PINN) stood out as it can exploit the underlying physics of engineering systems. The novelty of PINN lies in the use of partial differential equations (PDE) as regularizer loss.

Unlike deep learning [15] which requires training label for training the architecture, the regularizer in PINN does not require training labels. Instead, we train the regularizer loss in PINN similarly to a VAE's regularizer loss. Examples of neural networks using regularizer loss includes Autoencoder [16], Variational autoencoder (VAE) [17] and Generative adversarial net (GAN) [18]. A basic PINN architecture uses a standard multilayer perceptron (MLP). While VAE formulates the latent space of an Autoencoder using probability distributions, PINN formulates the output space of MLP using PDEs. We illustrate the loss functions of PINN in Fig. 1.

The PINN objective [1] seeks to minimize the losses incurred by i) mean-square error loss  $L_\mu$  and ii) physics-informed loss  $L_f$  as follows where  $\lambda$  is the tuning parameter.

$$L_{PINN} = L_\mu + \lambda L_f \quad (1)$$

### A. Mean square error loss

For Burger's equation, we refer to the input variables  $t$  and  $x$  as the time and sinusoidal axis in Fig. 4. The training dataset is defined as  $\chi = \{t_m, x_m\}_{m=1}^M$  and  $\hat{u} = \{\hat{u}_m\}_{m=1}^M$  for the input and output respectively for sample size  $M$ . For some multiphysics model e.g. Burger's equation, the training dataset can be obtained by generating dataset from initial condition and boundary conditions. For the  $b^{th}$  initial or boundary condition, the output function  $g_b$  and its inputs  $t_b, x_b$  are given as

$$\hat{u}_b = g_b |_{t_b, x_b} \quad (2)$$

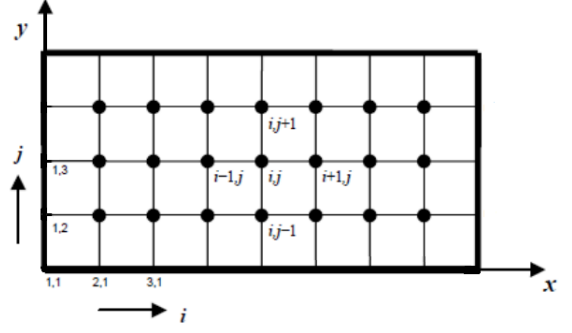


Figure 2. Approximating continuous electromagnetic field  $V_{(x,y)}$ , using a discrete 2D uniform grid of nodes  $\Gamma_{(i,j)}$ .

Whereas for Laplace's equation, we refer to the input variables as  $\chi = \{x_m, y_m\}_{m=1}^M$  and output variable  $\hat{V} = \{\hat{V}_m\}_{m=1}^M$  for the 2D electromagnetic field in Fig. 3.

The supervised learning part of PINN minimizes the Euclidean distance between ground truth  $\hat{V}$  and prediction  $V$  using mean square error (MSE) loss which is defined as (vice versa for  $\hat{u}$  and  $u$ )

$$L_\mu = \frac{1}{M} \sum_{m=1}^M |\hat{V} - V|^2 \quad (3)$$

### B. Physics-informed loss

For the unsupervised learning part of PINN, the physics-informed loss is a regularization that enforces PDE constraints on PINN by observing the prediction  $u$ . The PDE,  $f(u)$  captures the known underlying physics of an engineering system as studied by domain experts. The physics-informed loss is defined as

$$L_f = \frac{1}{M} \sum_{m=1}^M |f(u)|^2 \quad (4)$$

## III. PROPOSED METHOD

In this section, we mainly focus on the estimation of PDEs in physics-informed loss using numerical differentiation to reduce the complexity of training. In fact, numerical differentiation has been the de facto for multiphysics modeling for the past few decades and can be categorized into i) finite element method (FEM), ii) finite volume method (FVM), iii) finite difference method (FDM) and iv) boundary element method (BEM). Inspired by electromagnetic analysis [14], we propose to estimation PDEs using finite difference method (FDM). As mentioned earlier, our novelty is not about which numerical method is better e.g. FEM, FDM or FVM. Instead, our novelty lies in proposing the use of numerical differentiation for PINN over automatic differentiation [19].

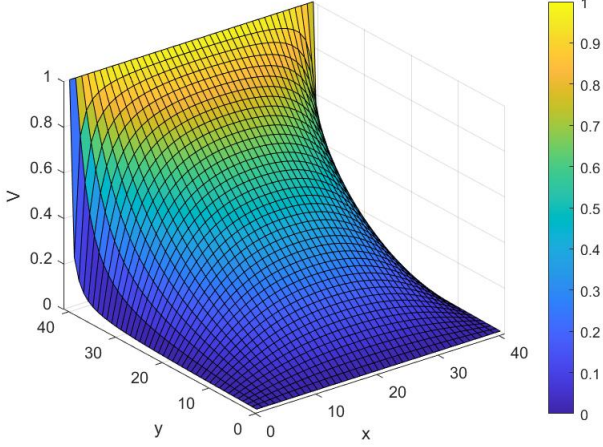


Figure 3. Plot of Laplace's equation (rectangular conducting trough) generated using SOR.

We demonstrate the proposed method on classical PDEs such as Laplace's and Burger's equations. The former is applied to electromagnetic systems and the latter can be found in fluid mechanics systems.

#### A. Laplace's Equation

In electromagnetic systems, the electromagnetic field is governed by Laplace's equation (in rectangular coordinates) in eqn (6). The estimation to Laplace's equation can be performed using a finite difference method in electromagnetic analysis known as the successive over-relaxation (SOR) algorithm [14]. The standard procedure for SOR is summarized as follows:

- i) Discretize a 2D uniform grid of nodes for representing the electromagnetic field  $V$
- ii) Slide the window computation of the residual  $R$  across each rows and columns.

Specifically, each iteration of SOR computes the residual  $R(i, j)$  per node, before applying an incremental update  $V_{new}(i, j)$  as follows

$$R(i, j) = \frac{1}{4} [V_{(i-1, j)} + V_{(i, j-1)} + V_{(i, j+1)} + V_{(i+1, j)}] \quad (5)$$

$$V_{new}(i, j) = V_{old}(i, j) + R(i, j)$$

Typically, SOR takes  $T$  numbers of iterations to converge. The number of  $T$  increases as the resolution of  $V(i, j)$  increases.

The rectangular conducting trough is an example of solving Laplace's equation (with Dirichlet boundary conditions in Table II) found in electromagnetic system [20]. The PDE (boundary conditions in Table II) is given as follows

$$f(V) = \frac{d^2V}{dx^2} + \frac{d^2V}{dy^2} \quad (6)$$

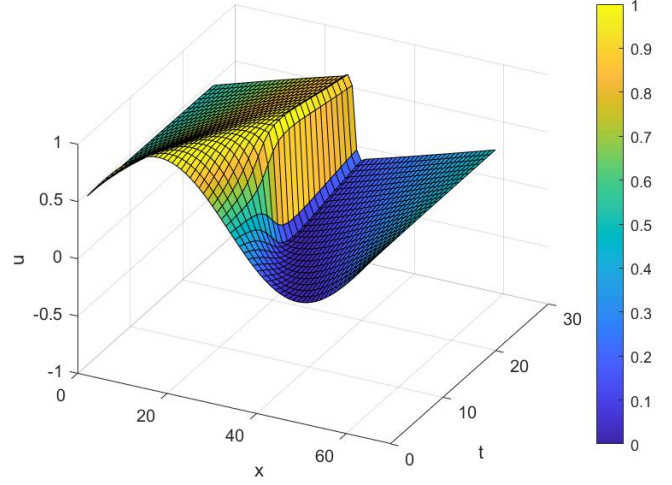


Figure 4. Plot of Burger's equation generated using "burgers\_shock.mat" [1].

When modeling  $f(V)$  as a physics-informed loss in Fig 2, it is non-trivial to define a closed form equation for backpropagation. Inspired by SOR where  $f(V)$  is approximated using a finite difference method (FDM) [14], we sought to apply FDM to physics-informed loss. First, we discretize  $f(V)$  over a grid of uniformly distributed nodes as shown in Fig. 1. Where  $h$  is the distance between each node. Next, we approximate  $f(V)$  in eqn (6) using FDM (in Table I) which becomes the following expression

$$\Gamma_{(i, j)} = \frac{V_{(i-1, j)} + V_{(i+1, j)} + V_{(i, j-1)} + V_{(i, j+1)} - 4V_{(i, j)}}{h^2} \quad (7)$$

We refers to  $\Gamma_{(i, j)}$  as the FDM of  $f(V)$  for a single node at  $(i, j)$ . We also note that eqn (7) is identical to SOR in eqn (5). Coincidentally,  $\Gamma_{(i, j)}$  resembles the Laplacian filter for edge detection in image processing.

#### B. Burger's Equation

We propose on how FDM can be applied to PINN for solving Burger's equation. The PDE of Burger's equation (boundary conditions in Table II) is defined as [1]

$$f(u) = u_t + uu_x - \left(\frac{0.01}{\pi}\right) u_{xx} \quad (8)$$

Since  $f(u)$  is intractable, most authors use automatic differentiation library e.g. "tf.gradients" or "dlgradient" in Table VI to handle the PDE computations. Instead, we propose to approximate  $f(u)$  using FDM. First we discretize the continuous time model  $u(x, t)$  by defining a 2D grid of uniformly spaced nodes over it. Next, we use FDM in Table I to approximate the first-order and second-order partial derivatives for the PDE. Thus, we arrive at the following equation

$$\Gamma_{(i,j)} = \frac{-3u_{(i,j)} + 4u_{(i,j+1)} - u_{(i,j+2)}}{2h}$$

$$+ u_{(i,j)} \left[ \frac{-3u_{(i,j)} + 4u_{(i+1,j)} - u_{(i+2,j)}}{2h} \right]$$

$$- (0.01/\pi) \frac{u_{(i-1,j)} - 2u_{(i,j)} + u_{(i+1,j)}}{h^2} \quad (9)$$

### C. PINN Weight Update

Once we have computed  $\Gamma_{(i,j)}$ , we can easily train PINN for both Burger’s and Laplace’s equation case. We seek to compute updates for the MLP weight,  $w_{j,j+1}$  using Stochastic Gradient Ascent (SGA) shown below and illustrated in Fig. 1

$$\Delta w_{j,j+1} = \gamma_\mu (\nabla L_\mu) + \lambda \gamma_f (\nabla L_f) \quad (10)$$

In eqn (10), the weight update of the hidden layers is defined as  $\Delta w_{j,j+1}$  for  $j = 1 \dots k$  number of hidden layers and learning rates  $\gamma_\mu, \gamma_f$ .  $\nabla L_\mu$  refers to the gradient of the MSE loss and closed form backpropagation is available [16]. On the other hand for the gradient of the PINN loss,  $\nabla L_f$  is non-trivial to compute. Thus, we propose to breakdown  $\nabla L_f$  using chainrule in eqn (11) to include the FDM term  $\Gamma$ , as previously introduced in eqn (7) and (9) for Laplace and Burger equation respectively

$$\nabla L_f = \frac{\delta L_f}{\delta \Gamma} \times \frac{\delta \Gamma}{\delta V} \quad (11)$$

In eqn (11),  $\delta L_f / \delta \Gamma$  is a differentiable term as  $L_f = \frac{1}{M} \sum_{m=1}^M |G|^2$  is a L2 regularizer loss. However,  $\delta \Gamma / \delta V$  represents the gradient of a local surface bounded by  $V_{(i,j)}$  and its neighboring nodes. For tractability, we further assume  $\delta \Gamma / \delta V$  is a constant.

## IV. EXPERIMENTS

In Table II, we refer to the PINN setup for modeling Laplace’s and Burger’s equation. The setup describes parameters for the continuous inputs and outputs, training dataset, initial / boundary conditions and their respective sample sizes ( $N_{ini}, N_{bc}$ ), collocation points ( $N_f$ ), loss functions, no. of neurons/ hidden layers and SGA parameters. We also restrict to lower collocation points to demonstrate the advantages of ND based PINN.

We perform the modeling tasks using:

- NN: training PINN using MSE loss  $L_\mu$  only.
- FDM-PINN (proposed): training PINN using  $L_{PINN}$  where physics-informed loss  $L_f$  is using finite difference method described in Section III.
- AD-PINN: training PINN using  $L_{PINN}$  where  $L_f$  is computed by automatic differentiation found in deep learning libraries e.g. Table VI.

Table I  
APPROXIMATING PARTIAL DIFFERENTIAL EQUATIONS USING FINITE DIFFERENCE METHOD.

First order PDE	$\frac{du}{dx} = \frac{-3u_{(i,j)} + 4u_{(i,j+1)} - u_{(i,j+2)}}{2h}$
Second order PDE	$\frac{d^2u}{dx^2} = \frac{u_{(i-1,j)} - 2u_{(i,j)} + u_{(i+1,j)}}{h^2}$

### A. Burger’s equation

The main difference between Burger’s and Laplace’s equation is the implementation of  $\Gamma_{(i,j)}$  in eqn (13) and (7). The minor differences are the parameters such as the network architecture, and grid size,  $N_{ini}$  and etc in Table II.

The ground truth (Fig. 4) for Burger’s equation is available online. We use a 64x25 grid for the ground truth. Our experiment is follows some of the setup in [1] where possible. We tabulate the average of 10 runs results for NN, AD-PINN and FDM-PINN and refer to the L2 error in Table II. Instead of computing L2 at every node, we use L2 to measure the full sinusoidal response between ground truth and PINN prediction at each time  $t$ . We then take the average of  $u(x,t)$  for all  $t$  as the error. In Table III, all methods suffer from larger error when training samples  $N_{ini}$  and  $N_{bc}$  are too low at 10 samples each. Both NN and FDM-PINN are implemented using eqn (11). The main difference between NN and FDM-PINN is the additional  $L_f$  term in eqn (9). Thus, we can find out how much  $L_f$  reduces the error. We observe that in fact FDM-PINN outperforms NN significantly. Both FDM-PINN and AD-PINN uses the same architecture setup and iterations ran and training samples counts. However, AD-PINN uses automatic differentiation for solving  $L_f$ ,  $L_\mu$  and the MLP. From the results, FDM-PINN is on par or better than AD-PINN for all training conditions. In terms of code execution time (Table V), FDM-PINN takes approximately 5X longer than NN to compute. Whereas, AD-PINN takes 5X longer than FDM-PINN, despite that AD-PINN uses a laptop based GPU whereas FDM-PINN and NN are computed using CPU. We suspect this could be due to the multiple AD operations required to run Burger’s equation as compared to the proposed FDM approach.

### B. Laplace’s equation

We use SOR to generate a 41x41 ground truth for the “rectangular conducting trough” in Fig. 3. The trough problem does not have a time variable like Burger’s equation. Instead, we have a 2D plane with surrounding boundary conditions [20]. Thus, we refer to  $N_{ini}$  instead as random subsamples from the ground truth.  $N_{bc}$  refers to random samples drawn from the 4 boundary conditions. Comparison of NN and PINN are made for fixed boundary condition sample size  $N_{bc}$  and varying initial sample size  $N_{ini}$  in Table III. We measure the L2 error between ground truth and PINN output for the entire grid. We tabulate the average of 10 runs results for

Table II  
EXPERIMENTAL SETUP

	Laplace's equation, $V(x, y)$	Burger's equation, $u(x, t)$
Continuous inputs and output	$x \in [0, 1], y \in [0, 1], V \in [0, 1]$	$x \in [-1, 1], t \in [0, 1], u \in [-1.0131, 1.0131]$
Ground truth	generated by SOR in eqn (6)	"burgers_shock.mat" [1]
# Nodes	$N_i \times N_j = 41 \times 41$	$N_i \times N_j = 64 \times 25$
Initial/Boundary conditions	$\hat{V}_1 = 0 \mid x_1=0, y_1=y$ $\hat{V}_2 = 0 \mid x_2=x, y_2=0$ $\hat{V}_3 = 0 \mid x_3=1, y_3=y$ $\hat{V}_4 = 1 \mid x_4=x, y_4=1$	$\hat{u}_1 = -\sin(\pi x) \mid x_1=x, t_1=0$ $\hat{u}_2 = 0 \mid x_2=-1, t_2=t$ $\hat{u}_3 = 0 \mid x_3=1, t_3=t$
Initial condition samples, $N_{ini}$	20, 30, 50, 100, 1000	10, 30, 50, 100
Boundary condition samples, $N_{bc}$	20	10, 30, 50, 100
Collocation points, $N_f$	1681	1600
Loss functions ( $\lambda = 0.7$ )	$L_{PINN} = L_\mu + \lambda L_f$	
Network architecture	2 - 50 - 50 - 50 - 1	2 - 30 - 30 - 30 - 1
Activation function	$\tanh$	
PINN learner	SGA with momentum	
Learning rates	$\gamma_\mu = 1e^{-1}, \gamma_f = 1e^{-3} \sim 1e^{-5}$	
Iterations ran	10,000	
minibatch size for $L_f$	32	8
minibatch size for $L_\mu$	4	8
Evaluation metric	$L2 = \sqrt{\sum_{j=1}^{N_j} \sum_{i=1}^{N_i} (V(\hat{i}, j) - V(i, j))^2}$	$L2 = \frac{1}{N_j} \sum_{j=1}^{N_j} \sqrt{\sum_{i=1}^{N_i} (u(i, j) - u(\hat{i}, j))^2}$

Table III  
MSE ON BURGER'S EQUATION

$N_{ini}$	10	30	50	100
$N_{bc}$	10	30	50	100
$N_f$	1600	1600	1600	1600
NN	2.0133	1.8493	1.6720	1.7107
AD-PINN	1.6450	<b>1.3291</b>	<b>1.3293</b>	1.4767
FDM-PINN	<b>1.5629</b>	1.3302	1.3426	<b>1.4153</b>

Table IV  
MSE ON LAPLACE'S EQUATION

$N_{ini}$	20	30	50	100	1000
$N_{bc}$	20	20	20	20	20
$N_f$	1681	1681	1681	1681	1681
NN	5.1164	4.8198	4.3277	4.0809	4.1246
AD-PINN	5.1946	4.8686	4.9758	4.5999	4.1131
FDM-PINN	<b>4.5782</b>	<b>3.6802</b>	<b>3.9836</b>	<b>3.4536</b>	<b>3.6162</b>

the NN, FDM-PINN and AD-PINN in Table IV. Firstly, we observe that a larger  $N_{ini}$  reduces the error for all methods. Secondly, we observe that NN and AD-PINN are quite similar in performance. However, AD-PINN suffers from poorer result between  $N_{ini}=50$  and  $N_{ini}=100$ . Overall, FDM-PINN outperforms both NN and AD-PINN significantly. The larger minibatch size for  $L_f$  as compared to  $L_\mu$  in Table II is found to empirically give a better result for FDM-PINN. However, the same setting did not appear to benefit AD-PINN. Also, increasing the minibatch size for  $L_\mu$  beyond 8 did not change

Table V  
EXECUTION TIME (PER ITERATION)

	Burger's Equation	Laplace's Equation
NN	0.0023 sec	0.0028 sec
AD-PINN	0.0478 sec	0.0653 sec
FDM-PINN	0.0097 sec	0.0609 sec

Table VI  
EXAMPLES OF USING AUTOMATIC DIFFERENTIATION FOR BURGER'S EQUATION

	Matlab	Tensorflow
$u =$	<code>model(parameters, x, t)</code>	<code>model(self, x, t, parameters)</code>
$u_x =$	<code>dlgradient(u, x)</code>	<code>tf.gradients(u, x)[0]</code>
$u_t =$	<code>dlgradient(u, t)</code>	<code>tf.gradients(u, t)[0]</code>
$u_{xx} =$	<code>dlgradient(u_x, x)</code>	<code>tf.gradients(u_x, x)[0]</code>

the result much for both NN, AD-PINN and FDM-PINN. In terms of execution time in Table V, FDM-PINN is slightly faster to compute than AD-PINN (with GPU). Due to the increase in hidden layers' neuron and minibatch size for  $L_f$ , FDM-PINN takes longer to compute Laplace's equation than previously for Burger's equation in Table V.

## V. CONCLUSION AND FUTURE WORK

Automatic differentiation is a modern deep learning black-box that enables PINNs to constraint the learning of neural networks with physics laws. On the other hand, numerical differentiation has always been the de facto PDE solver in mul-

tiphysics simulations for the past few decades. For instance, in electromagnetic analysis, the successive over-relaxation algorithm is a well known example of numerical differentiation that approximates the PDE of Laplace's equation.

In our work, we propose using numerical differentiation over automatic differentiation when training PINN. In our approach, we decouple the PDE solver from the PINN loss function such that it does not require automatic differentiation to be solved. Instead, we use numerical differentiation for the PDEs which in the Laplace's equation case is as simple as taking the average on the neighborhood of a node. This method can also be straightforward extended to the Burger's equation. We tested our proposed method (FDM-PINN) on both datasets of Laplace's and Burger's equation. We made comparison with the automatic differentiation based PINN. Our results under the condition of low collocation points showed that FDM-PINN is faster to compute while at least on par or better than automatic differentiation based PINN. However, one of main drawback FDM-PINN currently face is the need to define its collocation points on a grid. Secondly, we currently do not have a solution to compute the gradient of node surface i.e.  $\delta\Gamma/\delta u$ .

In future, we may consider a Markov-random field approach for the PDE solver since the PINN output is usually homogeneous. Another direction is to extend the PINN architecture to 2D such as the convolutional neural net.

## REFERENCES

- [1] M. Raissi, P. Perdikaris, and G. E. Karniadakis, "Physics-informed neural networks: A deep learning framework for solving forward and inverse problems involving nonlinear partial differential equations," *Journal of Computational Physics*, vol. 378, pp. 686–707, 2019.
- [2] L. Yang, D. Zhang, and G. E. Karniadakis, "Physics-informed generative adversarial networks for stochastic differential equations," *ArXiv*, vol. abs/1811.02033, 2020.
- [3] Y. Yang and P. Perdikaris, "Adversarial uncertainty quantification in physics-informed neural networks," *Journal of Computational Physics*, vol. 394, pp. 136–152, 2019.
- [4] W. Zhong and H. Meidani, "Pi-vae: Physics-informed variational auto-encoder for stochastic differential equations," *arXiv preprint arXiv:2203.11363*, 2022.
- [5] J. Kim, K. Lee, D. Lee, S. Y. Jin, and N. Park, "Dpm: A novel training method for physics-informed neural networks in extrapolation," *arXiv preprint arXiv:2012.02681*, 2020.
- [6] Z. Chen, Y. Liu, and H. Sun, "Physics-informed learning of governing equations from scarce data," *Nature communications*, vol. 12, no. 1, pp. 1–13, 2021.
- [7] R. G. Patel, I. Manickam, N. A. Trask, M. A. Wood, M. Lee, I. Tomas, and E. C. Cyr, "Thermodynamically consistent physics-informed neural networks for hyperbolic systems," *Journal of Computational Physics*, vol. 449, p. 110754, 2022.
- [8] K. He, X. Zhang, S. Ren, and J. Sun, "Deep residual learning for image recognition," in *Proceedings of the IEEE Conference on Computer Vision and Pattern Recognition*, 2016, pp. 770–778.
- [9] O. Hennigh, S. Narasimhan, M. A. Nabian, A. Subramaniam, K. Tangsali, Z. Fang, M. Rietmann, W. Byeon, and S. Choudhry, "Nvidia simnet: An ai accelerated multi-physics simulation framework," in *International Conference on Computational Science*. Springer, 2021, pp. 447–461.
- [10] T. Praditia, M. Karlbauer, S. Otte, S. Oladyskhin, M. V. Butz, and W. Nowak, "Finite volume neural network: Modeling subsurface contaminant transport," *arXiv preprint arXiv:2104.06010*, 2021.
- [11] Z. Fang and J. Zhan, "Deep physical informed neural networks for metamaterial design," *IEEE Access*, vol. 8, pp. 24 506–24 513, 2019.
- [12] Z. Fang, "A high-efficient hybrid physics-informed neural networks based on convolutional neural network," *IEEE Transactions on Neural Networks and Learning Systems*, pp. 1–13, 2021.
- [13] P.-H. Chiu, J. C. Wong, C. Ooi, M. H. Dao, and Y.-S. Ong, "Can-pinn: A fast physics-informed neural network based on coupled-automatic-numerical differentiation method," 2021.
- [14] J. R. Nagel *et al.*, "Solving the generalized poisson equation using the finite-difference method (fdm)," *Lecture Notes, Dept. of Electrical and Computer Engineering, University of Utah*, 2011.
- [15] A. Krizhevsky, I. Sutskever, and G. E. Hinton, "Imagenet classification with deep convolutional neural networks," in *Advances in neural information processing systems*, 2012, pp. 1097–1105.
- [16] G. E. Hinton and R. R. Salakhutdinov, "Reducing the dimensionality of data with neural networks," *science*, vol. 313, no. 5786, pp. 504–507, 2006.
- [17] D. P. Kingma and M. Welling, "Stochastic gradient vb and the variational auto-encoder," in *Second International Conference on Learning Representations, ICLR*, 2014.
- [18] I. Goodfellow, J. Pouget-Abadie, M. Mirza, B. Xu, D. Warde-Farley, S. Ozair, A. Courville, and Y. Bengio, "Generative adversarial nets," in *Advances in neural information processing systems*, 2014, pp. 2672–2680.
- [19] A. G. Baydin, B. A. Pearlmutter, A. A. Radul, and J. M. Siskind, "Automatic differentiation in machine learning: a survey," *Journal of Machine Learning Research*, vol. 18, pp. 1–43, 2018.
- [20] M. N. Sadiku and S. R. Nelatury, *Analytical Techniques in Electromagnetics*. CRC press, 2015.